Cell

An Assembly Chaperone Collaborates with the SMN Complex to Generate Spliceosomal SnRNPs

Ashwin Chari,[1] Monika M. Golas,[2] Michael Klingenhäger,[1] Nils Neuenkirchen,[1] Bjoern Sander,[2] Clemens Englbrecht,[1] Albert Sickmann,[3] Holger Stark,[2] and Utz Fischer[1,*]
[1]Department of Biochemistry, Biocenter, University of Würzburg, Am Hubland, D-97074 Würzburg, Germany
[2]Research Group of 3D Electron Cryomicroscopy, Max Planck Institute for Biophysical Chemistry, Am Fassberg 11, D-37070 Göttingen, Germany
[3]Rudolf Virchow Centre for Experimental Medicine, Versbacher Str. 9, D-97078 Würzburg, Germany
*Correspondence: utz.fischer@biozentrum.uni-wuerzburg.de
DOI 10.1016/j.cell.2008.09.020

SUMMARY

Spliceosomal small nuclear ribonucleoproteins (snRNPs) are essential components of the nuclear pre-mRNA processing machinery. A hallmark of these particles is a ring-shaped core domain generated by the binding of Sm proteins onto snRNA. PRMT5 and SMN complexes mediate the formation of the core domain in vivo. Here, we have elucidated the mechanism of this reaction by both biochemical and structural studies. We show that pICln, a component of the PRMT5 complex, induces the formation of an otherwise unstable higher-order Sm protein unit. In this state, the Sm proteins are kinetically trapped, preventing their association with snRNA. The SMN complex subsequently binds to these Sm protein units, dissociates pICln, and catalyzes ring closure on snRNA. Our data identify pICln as an assembly chaperone and the SMN complex as a catalyst of spliceosomal snRNP formation. The mode of action of this combined chaperone/catalyst system is reminiscent of the mechanism employed by DNA clamp loaders.

INTRODUCTION

Molecular chaperones interact transiently with polypeptide chains, prevent or reverse misfolding, and thereby promote the adoption of functional tertiary structures. The concept of chaperone action also applies to the assembly of multisubunit macromolecular complexes. In this case, the primary function is to orchestrate the joining of individual components into a higher-order complex. In addition, these chaperones prevent nonspecific or premature interactions. Examples for this type of chaperones (also termed assembly chaperones) include the biogenesis factors of nucleosomes, proteasomes, or Rubisco (Hirano et al., 2006; Laskey et al., 1978; Le Tallec et al., 2007; Saschenbrecker et al., 2007).

The enormous complexity of some ribonucleoprotein particles (RNPs) has implied that these macromolecular structures may, likewise, require assisting factors for their formation. In keeping with this notion, an active and factor-mediated process leads to the formation of the Sm class of spliceosomal small nuclear ribonucleoproteins (snRNPs) (Fischer et al., 1997; Meister et al., 2001a; Pellizzoni et al., 2002). This class, as an essential part of the spliceosome, catalyzes the removal of noncoding sequences from pre-mRNAs. SnRNPs are composed of a small eponymous snRNA, as well as common (Sm) and specific proteins. Prior to their involvement in the splicing cycle, snRNPs undergo a segmented biogenesis pathway, starting with the nuclear export of the snRNAs. Within the cytoplasm, the seven Sm proteins B-B′ (B′ is an alternatively spliced product of the Sm B gene), D1, D2, D3, E, F, and G bind to a single-stranded region of the RNA, termed Sm site. As a result, a toroidal Sm core domain is generated that interacts with the RNA in its central region (Kambach et al., 1999; Stark et al., 2001; Urlaub et al., 2001). After additional modification and processing steps, the RNP is targeted to its nuclear site of function (reviewed in Will and Lührmann, 2001).

The formation of the Sm core domain has been recapitulated in vitro with purified Sm proteins and snRNA (Raker et al., 1996). These studies have established a hierarchical maturation pathway in which Sm proteins initially form the three hetero-oligomers D3/B, D1/D2, and E/F/G independent of snRNA. Next, binding of D1/D2 and E/F/G onto the snRNA leads to the formation of an Sm subcore intermediate, which is finally converted into the mature Sm core upon the addition of the D3/B heterodimer. Even though self-recognition of RNA and protein counterparts is sufficient for Sm core assembly in vitro, two functional units, termed PRMT5 and SMN complexes (protein arginine methyltransferase 5 and survival motor neuron complexes), are required in vivo (Meister et al., 2002; Paushkin et al., 2002). The PRMT5 complex is composed of PRMT5, pICln, and WD45 (Mep50) and recruits Sm proteins via the pICln subunit (Friesen et al., 2001; Meister et al., 2001b). PRMT5 symmetrically dimethylates arginines (sDMA) within the C-terminal tail domains of Sm proteins B-B′, D1, and D3, which is believed to enhance their transfer onto the SMN complex (Brahms et al., 2001; Friesen and Dreyfuss, 2000). The SMN complex composed of

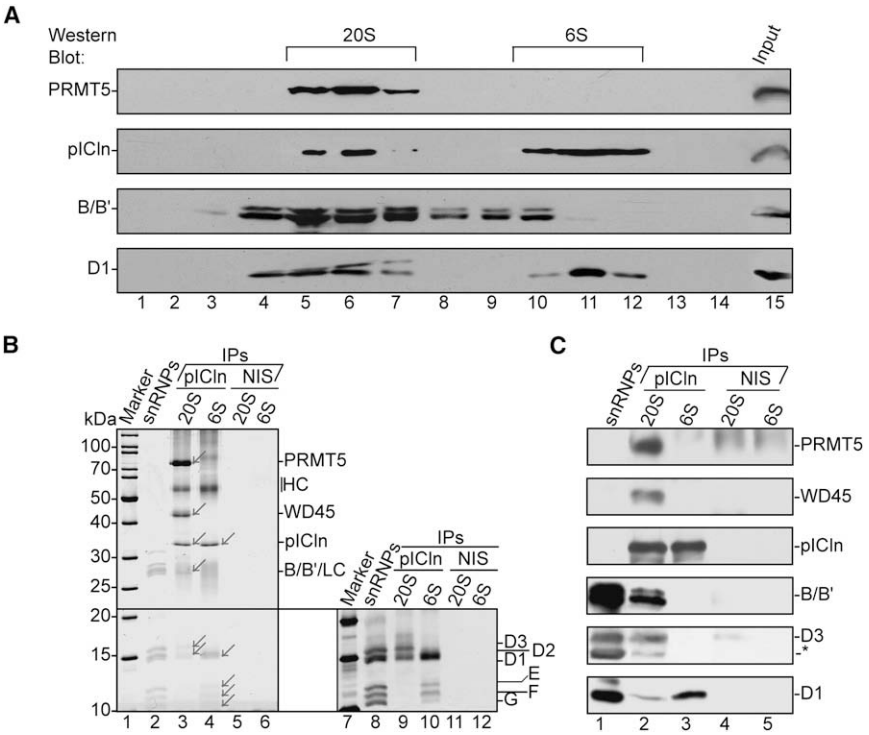

Figure 1. pICln Forms Two Complexes with Distinct Subsets of Sm Proteins

(A) Gel filtration fractions of HeLa cytosolic extract, active in snRNP assembly, were resolved by SDS-PAGE, and the indicated proteins were detected by western blotting. pICln was found in fractions corresponding to 20S (lanes 5–7) and 6S (lanes 10–12), respectively.

(B) Coomassie blue-stained gel of immunoaffinity-purified pICln complexes from the 20S (lane 3) and 6S (lane 4) fractions. Purifications with control antibodies are depicted in lanes 5 and 6, and a molecular size marker and affinity-purified snRNP cores are shown in lanes 1 and 2. The inset (lanes 7–12) shows a silver-stained portion of the same gel for a better visualization of low-molecular weight proteins.

(C) Western blot analysis of the immunoprecipitations (lanes 2–5) and affinity-purified snRNPs. The respective antigens were either detected with polyclonal antibodies (PRMT5, WD45, pICln) or the sDMA-specific monoclonal antibody Y12 (B/B′, D1, and D3). Asterisks mark nonspecific bands or degradation; HC and LC indicate heavy and light chains of the antibody used for affinity purification.

SMN and Gemins2–8 then facilitates the loading of Sm proteins onto snRNA, resulting in the formation of the Sm core (Gubitz et al., 2004; Meister et al., 2001a; Meister and Fischer, 2002; Neuenkirchen et al., 2008; Pellizzoni, 2007; Pellizzoni et al., 2002). Reduced expression of the SMN protein is the underlying cause for spinal muscular atrophy, providing an interesting link between the biogenesis of snRNPs and disease (Winkler et al., 2005; Zhang et al., 2008).

Although the factors that mediate Sm core formation have been identified, the mechanism of this reaction remains elusive. Here, we have dissected the assembly process by a combination of biochemical and structural studies. We identify a ring-shaped 6S particle composed of the Sm proteins D1/D2, E/F/G, and pICln, which does not allow RNA binding. SnRNP core formation depends on the activity of the SMN complex, which contacts the outer surface of this 6S intermediate and displaces pICln. As a consequence, the Sm proteins adopt an arrangement ready for snRNA binding and RNP formation. Our data identify pICln as an Sm-specific assembly chaperone and the SMN complex as a catalyst for the transfer of Sm proteins from the 6S complex onto snRNA.

RESULTS

pICln Is a Constituent of Two Complexes, Each Containing Distinct Subsets of Sm Proteins

Previous studies have demonstrated a direct interaction between pICln and Sm proteins that occurs in Sm core formation before the SMN complex is involved (Friesen et al., 2001; Meister and Fischer, 2002). To understand its role in the biogenesis pathway, we set out to identify complexes formed between pICln and Sm proteins in steady state. When cytosolic extract from HeLa cells was size fractionated by gel filtration, pICln eluted in two peaks that correspond to approximate sedimentation values of 20S and 6S, respectively (Figure 1A; see Supplemental Data available online for transformation of molecular weight into sedimentation values). The Sm protein D1 had an elution profile very similar to pICln, whereas PRMT5 and B-B′ were predominantly found in the 20S peak. Both peak fractions were individually subjected to immunoaffinity purification with anti-pICln antibodies and analyzed by SDS-PAGE, western blotting, and mass spectrometry. These approaches resolved the 20S peak as a complex formed by pICln, PRMT5, WD45, and all Sm proteins (Figures 1B, lanes 3 and 9, and 1C, lane 2). Of note, E/F/G in this peak was consistently underrepresented when compared to the other Sm proteins and, in many cases, could only be detected by mass spectrometric analyses (see also Figure S1). The 6S peak fraction, aside from pICln, contained the Sm proteins D1/D2 and E/F/G in apparently stoichiometric amounts while being devoid of D3/B (Figures 1B, lanes 4 and 10, and 1C, lane 3). Furthermore, immunoblots with the symmetrical dimethylarginine-specific Sm antibody Y12 revealed that not only the Sm proteins D1, D3, and B of the 20S complex were methylated, but also D1 in the 6S complex (Figures 1A, 1C, and data not shown). Thus, upon size fractionation, pICln resolves into two peaks, one containing only the Sm proteins of the snRNP subcore (6S) and one that is equivalent to the previously identified PRMT5 complex (20S).

An Ordered Sequence of Events Leads to the Formation of the 6S Complex

Isolated 6S complex contains equimolar quantities of D1, D2, E, F, G, and pICln (Figure 1B, lanes 4 and 10). However, the Sm

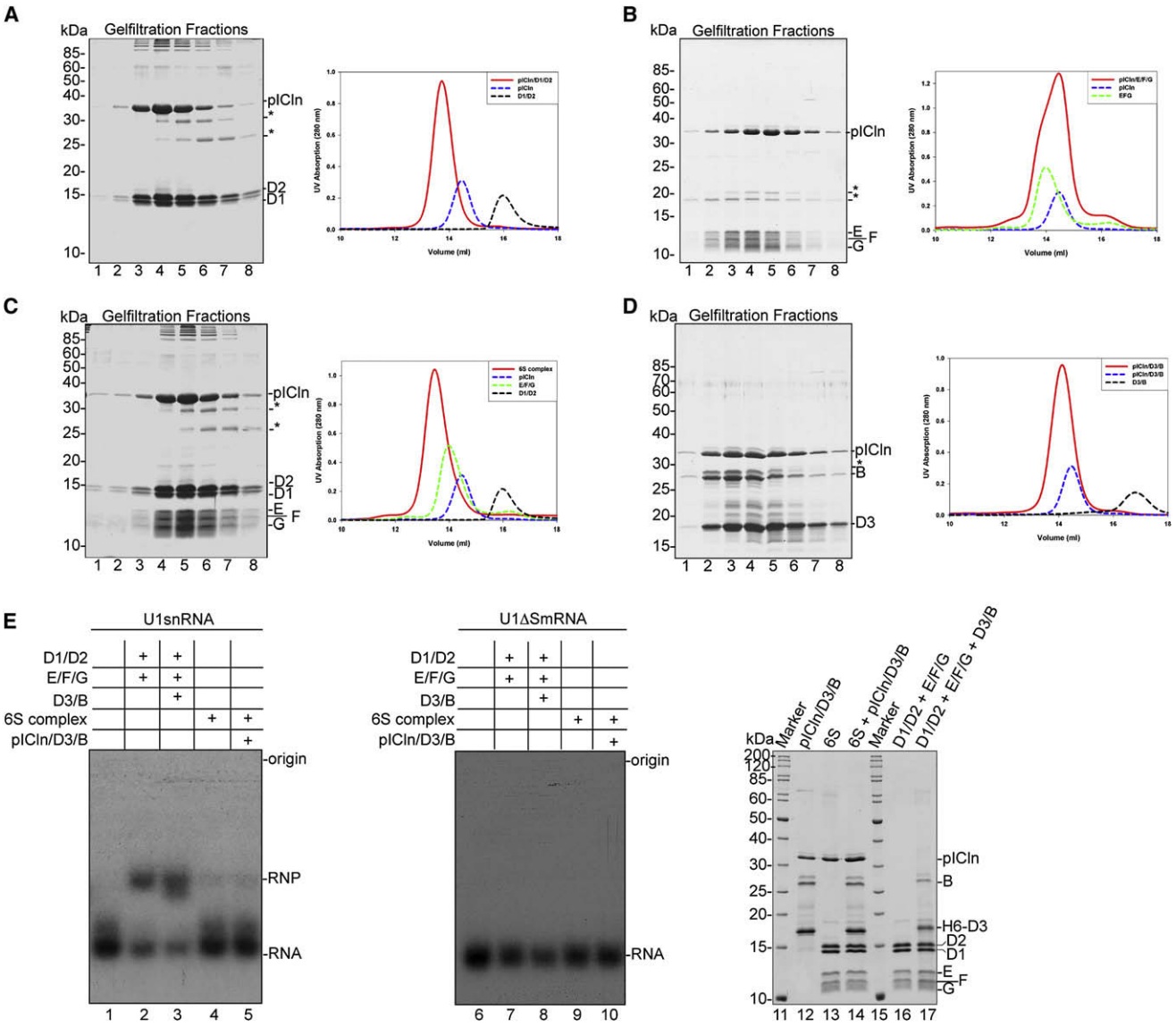

Figure 2. Cooperative Binding of Sm Proteins to pICln Leads to the Formation of an Assembly-Inactive 6S Complex

Recombinant pICln was incubated with equimolar amounts of D1/D2 (A), E/F/G (B), a combination of D1/D2 and E/F/G (C), or D3/B (D). The mixtures were separated by gel filtration, and individual fractions were analyzed by SDS-PAGE (left panel). Chromatograms of the mixtures and of individual building blocks, respectively, are shown (right panel). Asterisks denote impurities. (E) In vitro assembly of ^{32}P-labeled U1snRNA with either isolated Sm protein hetero-oligomers (lanes 2 and 3) or pICln-Sm complexes (lanes 4 and 5). RNP formation was analyzed by native gel electrophoresis. U1snRNA without proteins is shown in lane 1. In lanes 6–10, the same experiment was performed with U1ΔSm. Lanes 12–14, 16, and 17 depict the complexes used for these experiments.

protein units D1/D2 and E/F/G alone are incapable of forming a stable complex in the absence of snRNA (Raker et al., 1996). Therefore, we determined in detail how the five Sm proteins interact with pICln to form the 6S complex. For this, we incubated pICln with equimolar amounts of recombinant and unmethylated D1/D2, E/F/G, or a combination of both. Complex formation was monitored by gel filtration and subsequent SDS-PAGE. pICln formed a homogenous complex with D1/D2, as evident by the strict coelution of the three proteins in identical fractions from the column (Figure 2A). In contrast, in the presence of pICln, E/F/G eluted as a separate entity, indicating no or inefficient complex formation (Figure 2B; see also the chromatograms of individual components in the right panel). However, when pICln was incubated with a mixture of the Sm hetero-oligomers D1/D2 and E/F/G, a stable complex was formed (Figure 2C) with an identical elution profile to the 6S complex presented in Figure 1A. These findings are corroborated by immunoprecipitation of individual gel filtration fractions with anti-pICln antibodies (data not shown). Thus, the 6S complex forms in a stepwise manner, and the binding site for the E/F/G heterotrimer is generated by the preceding formation of a pICln/D1/D2 trimer. These data also suggest that methylation of Sm D1 appears to be dispensable for 6S formation.

pICln formed a second stable unit with the unmethylated D3/B hetero-oligomer, i.e., the Sm proteins missing in the 6S complex (Figure 2D). Interestingly, the pICln/D3/B complex failed to interact with any of the other two Sm hetero-oligomers and, hence, is a separate unit (data not shown). This pICln complex is not detected at steady state in size-fractionated cytosolic extracts (see Figure 1A and data not shown) and, hence, is likely to be either short lived or to exist only as part of the 20S PRMT5 complex.

Sm Proteins Do Not Associate with SnRNA in a pICln-Bound Form

The 6S complex (pICln/D1/D2/E/F/G) contains the five Sm proteins required for the assembly of the snRNP subcore, i.e., the intermediate formed in vitro on snRNA in the absence of the D3/B heterodimer (Raker et al., 1996). This raised the question of whether the Sm proteins of the 6S complex were able to associate with snRNA. By native gel electrophoresis, we demonstrate that neither preformed 6S complex alone nor in conjunction with the pICln/D3/B heterotrimer forms RNPs on ^{32}P-labeled U1snRNA (Figure 2E, lanes 4 and 5). In contrast and consistent with a previous report (Raker et al., 1996), spontaneous formation of the Sm subcore was observed upon incubation of D1/D2 and E/F/G with U1snRNA, which is matured into the snRNP core upon addition of D3/B (Figure 2E, lanes 2 and 3). No RNPs were formed on RNA lacking a functional Sm site either with pICln-bound or free Sm proteins (Figure 2E, lanes 6–10; see lanes 12–14, 16, and 17 for the protein complexes used). Therefore, Sm proteins appear to be incompetent to form snRNPs when they are associated with pICln. This could either mean that the 6S complex is a dead-end product in the assembly pathway or that it acts as a kinetic trap for the bound Sm proteins. If the latter scenario was correct, pICln would be a reversible inhibitor of snRNP core formation. This calls for another factor to liberate Sm proteins from the pICln-imposed inhibition and render them competent to form snRNPs.

Concurrent Transfer of Sm Proteins onto the SMN Complex and Dissociation of pICln

As the SMN complex is known to promote snRNP assembly in vivo (Massenet et al., 2002; Meister et al., 2001a; Meister and Fischer, 2002; Pellizzoni et al., 2002; Shpargel and Matera, 2005), we speculated that it might relieve Sm proteins from the pICln-induced inhibition. We addressed this hypothesis by incubating preformed recombinant 6S and pICln/D3/B complexes with immobilized, affinity-purified SMN complexes (see Figure 3A for protein compositions of the complexes involved). After extensive washing, the retained proteins were analyzed by SDS-PAGE and western blotting. As shown in Figure 3B, Sm protein transfer occurred efficiently in both cases, as evident by an increase of the respective Sm protein levels on the SMN complex (Figure 3B, lanes 3, 4, 7, and 8, and S2; note that Sm B comigrates with the light chain of the antibody). This reaction was strictly dependent on the SMN complex and could not be observed on a control column (Figures 3B, lanes 23 and 24, and S3, lanes 11 and 12). Furthermore, we found that the transfer reaction did not require prior methylation of Sm proteins, as these were obtained by bacterial expression.

Next, we addressed whether the tail domains of Sm proteins, i.e., the sites of sDMA modification were required for SMN complex binding. For this, we performed the transfer reaction with a reconstituted pICln/D3/B complex in which the tail domains of both Sm proteins were absent (referred to as pICln/D3-Sm/B-Sm). The SMN complex efficiently accepted this truncated D3/B heterodimer, comparable to the Sm proteins of the 6S complex (Figure S3, lanes 3, 4, 7, and 8). Having established that Sm proteins are transferred from pICln complexes to the SMN complex irrespective of their methylation status, we analyzed the fate of pICln in this reaction. By western blotting, pICln was shown to be absent from the recipient SMN complex, suggesting its dissociation from Sm proteins during transfer (Figures 3B, lanes 3 and 4, and S3, lanes 3 and 4, pICln immunoblot panel in the bottom of the figure).

We next asked which subunits of the SMN complex participated in the Sm protein transfer reaction. As a prerequisite to address this question, we expressed two recombinant SMN complexes that lack Gemins 3, 4, and 5 (SMNΔGemin3–5) or Gemins 3, 4, 5, 6, and 7 (SMNΔGemin3–7) and purified them to near homogeneity (Figure 3A; see Supplemental Data for details). These units were immobilized onto an anti-SMN antibody resin, and transfer reactions were performed as described. Surprisingly, both units took over the Sm proteins in a manner indistinguishable from the endogenous complex, concurrent with the dissociation of pICln (Figure 3B, lanes 11, 12, 15, and 16). Hence, loading of the SMN complex with Sm proteins does not require Gemins 3–7.

However, when the SMN complex was further reduced to a heterodimer composed of Gemin2 and an N-terminal fragment of SMN containing residues 1–160 (termed Gemin2/SMNΔC), the transfer reaction was stalled at an intermediate stage. Although Gemin2/SMNΔC still interacted with the 6S complex, the extent of pICln dissociation was reduced (see arrow in Figure 3B, lane 19 and pICln Immunoblot panel). In fact, this stalled transfer intermediate was stable and could be reconstituted with the recombinant proteins pICln, Gemin2/SMNΔC, D1/D2, and E/F/G (Figure S4, hereafter referred to as the 8S complex). Furthermore, transfer of the Sm proteins D3/B from pICln onto the Gemin2/SMNΔC heterodimer was severely impaired (Figure 3B, lane 20). Taken together, these experiments reveal that a heterotrimeric complex composed of SMN, Gemin2, and 8 is sufficient to accept all seven Sm proteins from pICln. However, the simultaneous removal of Gemin8 and the C-terminal part of SMN from this minimal system reduces the capacity to dissociate pICln from Sm proteins and recruit the Sm proteins D3/B.

Reversal of a Kinetic Trap upon Transfer of Sm Proteins from 6S onto the SMN Complex

The findings above show that Sm proteins are incapable of associating with RNA while bound to pICln (Figure 2E). The activity of the SMN complex, in turn, leads to the displacement of pICln (Figure 3B). Hence, we considered that this activity is a major prerequisite for the subsequent formation of snRNPs. In a first approach, we analyzed the assembly of U1snRNP in the presence of endogenous SMN complex affinity purified from cytosolic extract. As this complex is active per se (Figure 4A,

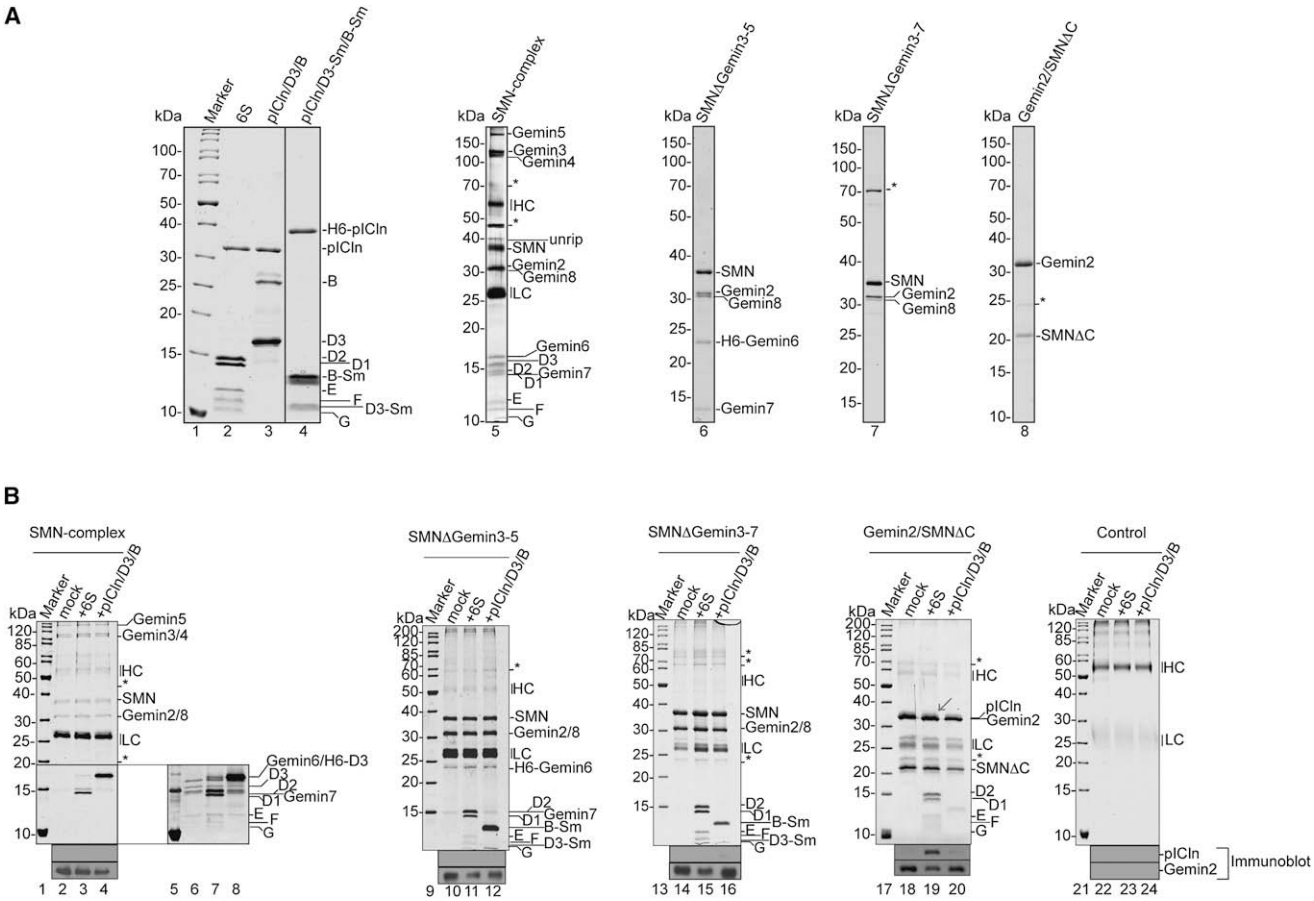

Figure 3. Transfer of Sm Proteins from pICln onto the SMN Complex

(A) SDS-PAGE of protein complexes used for the transfer reactions: recombinant 6S (lane 2), pICln/D3/B (lane 3), and pICln/D3-Sm/B-Sm (lane 4) complexes. Lane 5 shows affinity-purified endogenous SMN complex. Lanes 6–8 show the recombinant SMN subcomplexes SMNΔGemin3–5 (lane 6), SMNΔGemin3–7 (lane 7), and Gemin2/SMNΔC. Bands marked with an asterisk indicate nonspecific proteins; HC and LC indicate heavy and light chains of the antibody used for affinity purification.

(B) Transfer of Sm proteins from pICln complexes to the SMN complex. The respective, immobilized complexes (labeled on top) were incubated with either the 6S complex (lanes 3, 7, 11, 15, and 19), pICln/D3/B (lanes 4, 8, 12, 16, and 20), or treated with buffer only (lanes 2, 6, 10, 14, and 18). A control purification from HeLa extract was incubated with the 6S complex (lane 23), pICln/D3/B (lane 24), or buffer (lane 22) as a control. Proteins retained on the resin were analyzed by SDS-PAGE and western blotting with anti-pICln and anti-Gemin2 antibodies.

lane 4), a preincubation with a large molar excess of nonlabeled U1snRNA was performed to exhaust its inherent assembly activity (see Figure S5 for details). SMN complex treated this way failed to promote the formation of snRNPs on ^{32}P-labeled U1snRNA (Figure 4A, lane 2). However, a simultaneous preincubation of the activity depleted SMN complex with 6S complex, and pICln/D3/B led to its reactivation and enabled assembly of the Sm core domain on U1snRNA (Figure 4A, lane 3). No RNPs were formed on U1snRNA lacking the Sm site (U1ΔSm) (Figure 4A, lanes 5–8).

Next, the same reaction was performed with recombinant SMNΔGemin3–5 and SMNΔGemin3–7 complexes. As shown in Figures 4B and 4C, both failed to assemble U1snRNPs when Sm proteins were lacking (lanes 2). However, when loaded with 6S and pICln/D3/B or with 6S alone, they induced assembly of Sm cores and subcores, respectively (Figures 4B and 4C, lanes 3 and 4). No assembly was observed when the complexes were loaded with either pICln/D3/B alone (Figures 4B and 4C, lanes 5) or when any of the complexes were incubated with U1ΔSm (Figures 4B and 4C, lanes 6–10). Thus, along with experiments described in Figure 3B, we conclude that Sm proteins regain the competence to form snRNPs as a consequence of their transfer onto the SMN complex and the concomitant dissociation of pICln.

In contrast, we failed to activate the minimal Gemin2/SMNΔC dimer for snRNP assembly upon incubation with either 6S or pICln/D3/B complex (Figure 4D, lanes 2–4). As described in Figure 3B, the incubation of Gemin2/SMNΔC with the 6S complex results in a stalled transfer reaction intermediate. We hypothesized that removal of pICln would resolve this stalled state and enable Sm subcore formation. To address this, a complex composed of Gemin2/SMNΔC/D1/D2/E/F/G was reconstituted from recombinant proteins (Figure S6, hereafter referred to as the 7S complex). Indeed, this complex promoted efficient

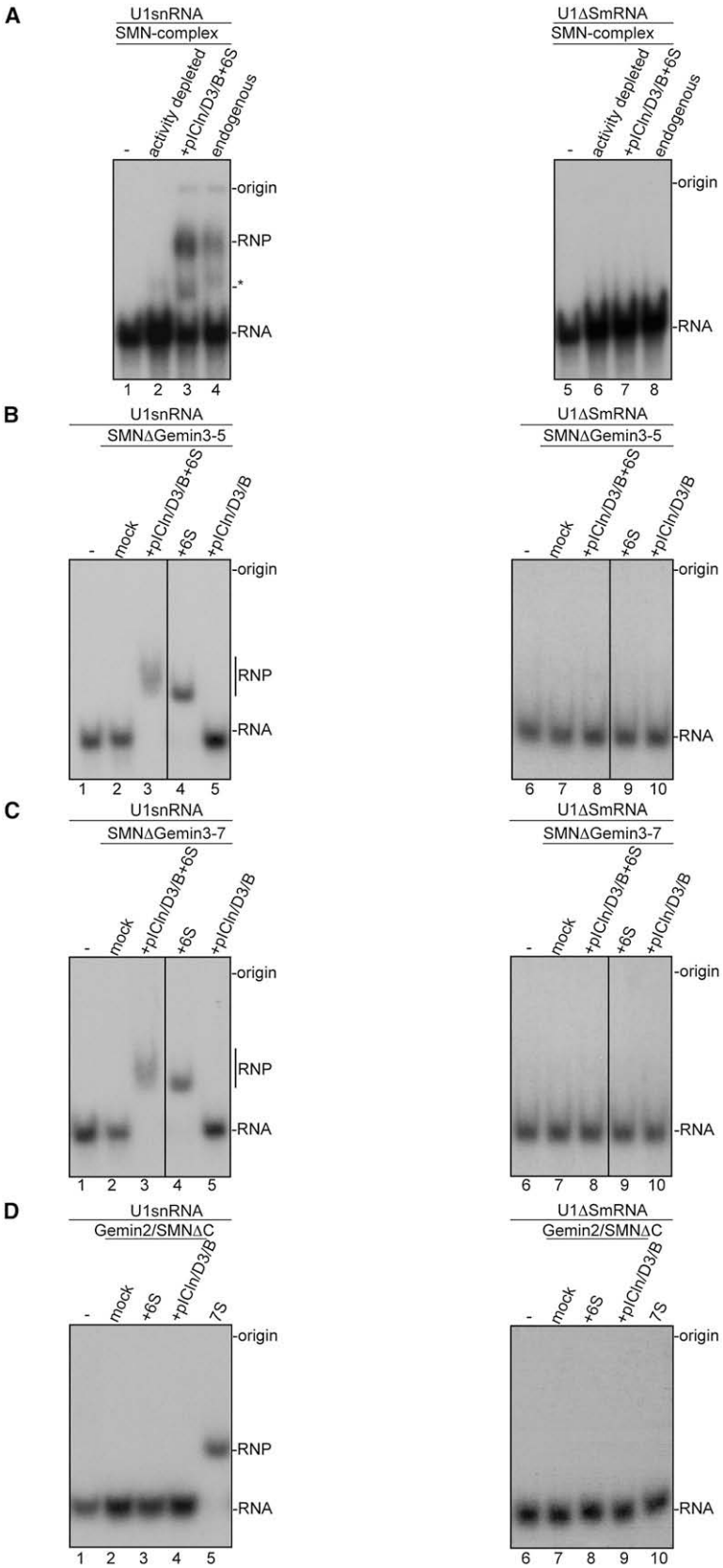

Figure 4. SnRNP Core Formation Correlates with the Capability of the SMN Complex to Dissociate pICln from Sm Proteins

(A) Immobilized, affinity-purified SMN complex was either mock treated ("endogenous") or incubated with an excess of unlabeled U1snRNA to exhaust its assembly capacity ("activity-depleted"). After washing, both complexes were incubated with ^{32}P-labeled U1snRNA, and complex formation was analyzed by native gel electrophoresis (lanes 2 and 4). In lane 3, activity-depleted SMN complex was incubated with 6S and pICln/D3/B complexes and washed before addition of ^{32}P-labeled U1snRNA. Lanes 5–8 show control reactions on ^{32}P-labeled U1ΔSmRNA; lanes 1 and 5 show RNA only. The band marked with "RNP" corresponds to the Sm core; the asterisk denotes an RNP lacking Sm proteins.

(B) Assembly reactions on ^{32}P-labeled U1snRNA with recombinant SMNΔGemin3–5 complex without bound Sm proteins (lane 2) or loaded with the indicated pICln-Sm complexes (lanes 3–5). Lane 1 shows RNA only; lanes 6–10 show control assembly reactions on ^{32}P-labeled U1ΔSmRNA.

(C) Assembly reactions as in (B) but with SMNΔGemin3–7.

(D) Assembly reaction as in (B) using the Gemin2/SMNΔC dimer without Sm proteins (lanes 2 and 7) or preincubated with 6S (lanes 3 and 8) and pICln/D3/B (lanes 4 and 9), respectively. An in vitro reconstituted complex composed of Gemin2/SMNΔC/D1/D2/E/F/G was incubated with U1snRNA (lane 5) or U1ΔSmRNA (lane 10) prior to native gel electrophoresis.

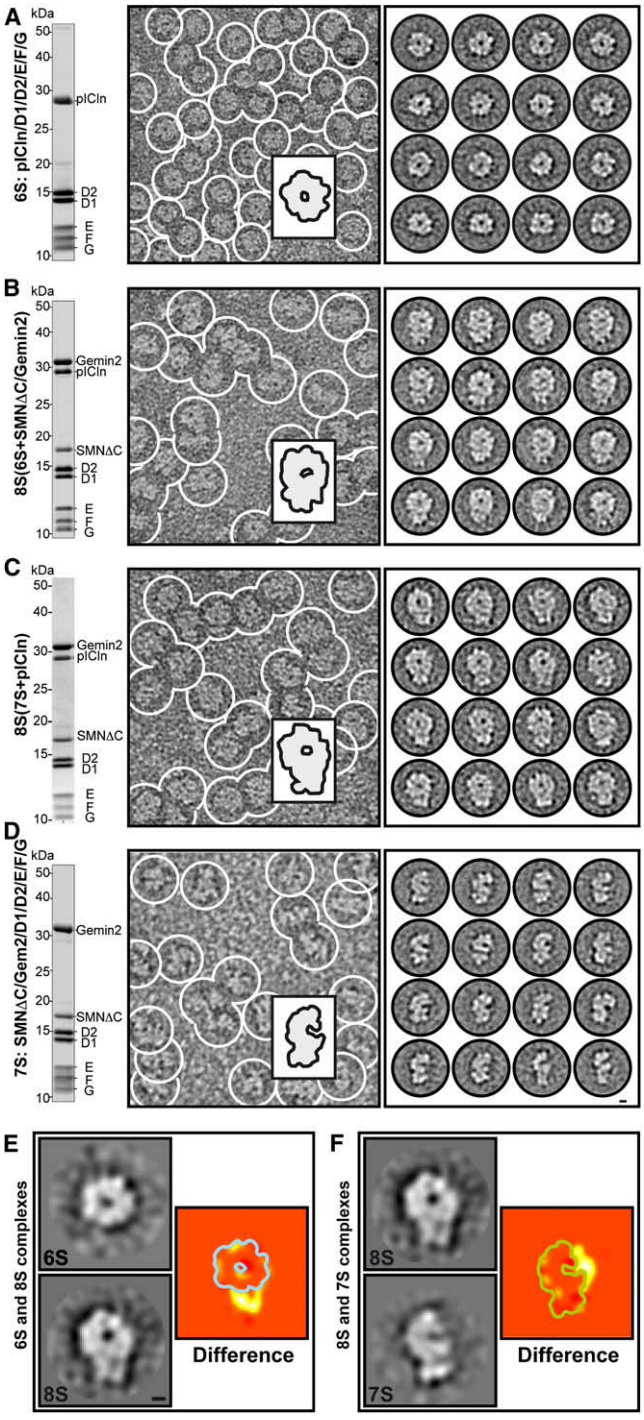

Figure 5. Electron Microscopic Analysis of Assembly Intermediates

(A–D) Reconstituted assembly intermediates (for SDS-PAGE of the respective complexes, see left panel) were subjected to EM analysis: (A) 6S, (B) and (C) 8S, and (D) 7S complexes. Note that the 8S complex was either reconstituted by incubating 6S complexes with SMNΔC/Gemin2 (B) or adding pICln to 7S complexes (C). Characteristic raw images and class averages of assembly intermediates are shown in the middle and right panel, respectively. The insets depict a schematic representation of particle morphology.

assembly of the Sm subcore in a strictly Sm site-dependent manner (Figure 4D, lanes 5 and 10). From these experiments we conclude that Sm core formation directly correlates with the capability of the SMN complex to dissociate pICln from the Sm proteins. Furthermore, assembly of the Sm core per se requires only a minimal set of subunits of the SMN complex in vitro, namely SMN and Gemin2. Our recent finding of a minimal SMN complex in *Drosophila melanogaster* composed of the same two proteins further corroborates the latter conclusion (Kroiss et al., 2008 and Supplemental Discussion).

Structural Analysis of Assembly Intermediates Suggests a Mechanism for SnRNP Core Formation

As both the 6S (pICln/D1/D2/E/F/G) and 7S (Gemin2/SMNΔC/D1/D2/E/F/G) complexes contain the same set of Sm proteins, it was intriguing to ask what makes the first one incompetent and the latter suitable for Sm subcore formation. We reasoned that the transition from the inactive to an activated state is accompanied by structural rearrangements. To address this, we conducted electron microscopic (EM) studies of the reconstituted 6S complex; the stalled Sm protein transfer intermediate from 6S to SMN complexes, designated as the 8S complex (Gemin2/SMNΔC/pICln/D1/D2/E/F/G); and the 7S complex as a subunit of the SMN complex functional in RNP formation. Due to their decreased susceptibility to proteolysis, we turned to the highly homologous *Drosophila* counterparts of the respective complexes. As shown in Figures 5A–5D, left panel, these complexes could be efficiently reconstituted from single proteins and purified to homogeneity. Gel filtration of these complexes indicated molecular masses consistent with a monomeric stoichiometry of each constituent. Moreover, the *Drosophila* complexes conform to the identical biochemical characteristics described above for their respective human counterparts (data not shown).

Typical negatively stained EM fields of all three purified, reconstituted complexes revealed a monodisperse population of asymmetric single particles with well-defined, distinct structural features (Figures 5A–5D, middle panels). All four analyzed data sets (6S, 8S[6S+SMNΔCGemin2], 8S[7S+pICln], 7S particles) showed preferential binding orientation of the particles on the carbon film (87%–94% of the particle views; see Figure S7 for details). Class averages of the 6S complex exhibit a ring-like architecture with a central accumulation of stain (Figure 5A, middle

(E and F) Difference maps identify shared structural elements and lacking domains in the Sm-containing complexes. The shapes of the respective complexes are shown on the left side and the difference maps on the right side of each panel. Differences are visible as bright yellow regions within the map. For comparison, the contours of the 6S (blue) and 7S (green) complexes are also drawn in the difference maps.

(E) A comparison of the 6S complex and the 8S transfer intermediate complex reveals shared features in the ring-shaped domain, while the foot-like domain of the 8S intermediate complex is lacking in the 6S complex. This suggests that SMN and Gemin2 form the foot-like domain.

(F) Difference map of the 8S transfer intermediate and the 7S complex shows common features in most parts of both ring-shaped and foot-like domains, while a minor portion of the ring-like domain is missing in the 7S complex. This suggests that pICln is located within the ring-like density element. Scale bar, 2 nm.

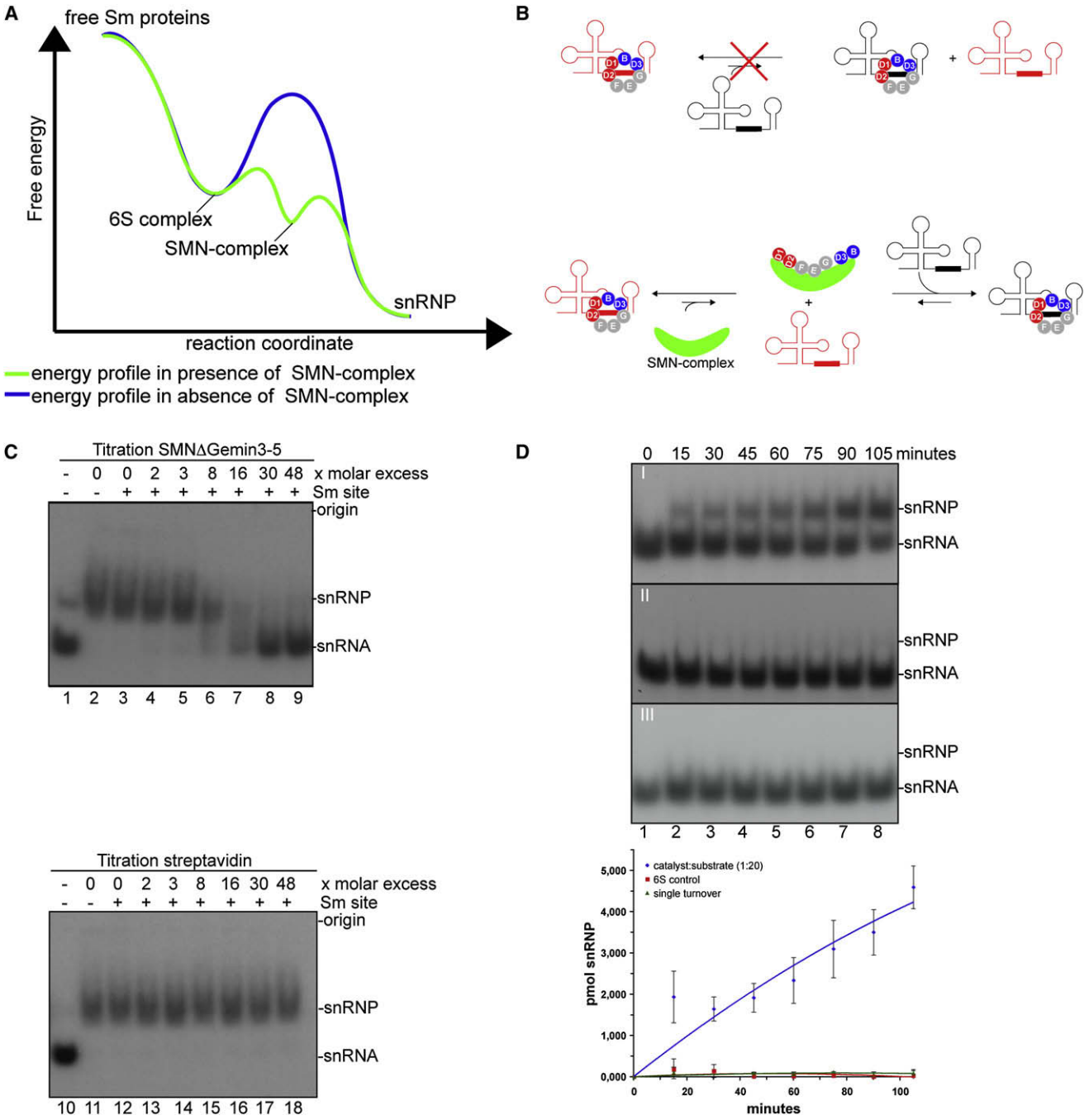

Figure 6. The SMN Complex Is a Catalyst of SnRNP Core Formation

(A) Hypothetical energy profile of snRNP core formation in vivo in the absence (blue line) and presence (green line) of the SMN complex. The model suggests that formation of the 6S complex results in a kinetic trap for Sm proteins and that the SMN complex acts as a catalyst for the transition from the 6S complex to the snRNP.

(B) Schematic of the experimental setup to test whether the SMN complex is a catalyst. Due to the stability of the Sm core domain, transfer of Sm proteins from an assembled core (red RNA) onto unlabeled competitor snRNA (black) is unlikely (upper panel). The hypothesized role of the SMN complex as a catalyst is illustrated in the lower panel.

(C) ^{32}P-labeled U1snRNA (lane 1) was incubated with Sm proteins to allow formation of the Sm core domain (lane 2). To the preformed core, a 330-fold molar excess of Sm-site RNA and increasing amounts of SMNΔGemin3–5 were added (lanes 3–9). The reactions were resolved on native gels 2.5 hr later. The same reactions were performed in the presence of increasing amounts of streptavidin instead of the SMNΔGemin3–5 complex (lanes 10–18).

(D) Panel I depicts RNP formation at the indicated time points with 10 pmol each of the 6S complex and RNA and 0.5 pmol of the SMNΔGemin3–5 complex (a catalyst:substrate ratio of 1:20). Panel II shows assembly of 10 pmol U1snRNA and 0.5 pmol SMNΔGemin3–5 complex preloaded with the Sm proteins D1/D2

and right panels). These particles had a maximum diameter of about 8–8.5 nm. Notably, these dimensions are comparable to those reported for the Sm core domain (Kastner and Lührmann, 1989). In contrast, the shape of assembly active 7S complexes was strikingly different (Figure 5D, middle and right panels). Class averages showed elongated particles with a length of about 11.5 nm. Importantly, the closed ring observed in 6S complexes was now converted into an open clamp (upper domain), which is packed against a foot-like protuberance (lower domain). Thereby, the opening of the clamp (oriented to the right side in Figure 5D) was found in proximity to the foot-like domain. The transfer intermediate 8S complex still contained the ring shape of the 6S complex (upper domain) but displayed, additionally, a foot-like protuberance as the 7S complex (lower domain) (Figures 5B and 5C, middle and right panels). Notably, the ring domain of this particle had a diameter of about 8–8.5 nm and, hence, has very similar dimensions as the 6S complex. The overall length of these particles was about 11.5 nm, similar to that of 7S complexes. To investigate whether the closed and open states are the result of different conformations or of different orientations on the carbon film, we also tilted the specimen in the electron microscope. In support of our model, this did not change the open or closed appearances of individual particles (data not shown).

Since the 8S complex comprises both structural features of 6S and 7S complexes and all three complexes contain the five Sm proteins D1, D2, E, F, and G as a common compositional denominator, we determined the positions of accessory factors by structural comparison. In particular, the similarity of distinct domains is not only restricted to the overall shape, but is also seen in fine structural details. All four samples were analyzed independently of the respective other three to enable an unbiased structural characterization of the complexes. Two-dimensional difference maps of the complexes elucidated shared structural elements as well as differences (Figures 5E and 5F). 6S and 8S complexes share the globular ring-like domain (Figure 5E; for comparison, the shape of the 6S complex is shown as a blue line in the difference map). We noted minor changes in the ring-like domain, which most likely represent conformational changes or slightly varied projections and large deviances in the foot-like protuberance of the 8S complex (yellow regions). We attribute the latter to a compositional difference and, therefore, suggest that the foot-like domain is the position of Gemin2 and SMNΔC, as these two proteins are the only ones lacking in the 6S complex.

Difference maps of the 8S intermediate and the 7S complex showed common structural elements in the majority of the ring-like upper domain and foot-like domain in the lower region of the complex (Figure 5F). A minor portion of the circular domain, however, is missing in the 7S complex, suggesting that this is the position occupied by pICln, which is the compositional difference between the 8S and 7S complex (Figure 5F; for comparison, the contour of the 7S complex is shown as a green line in the difference map). We also observed small differences along the body of the particle, which we yet again attribute to conformational changes or slightly different adsorption orientations on the EM grid. Therefore, we suggest that pICln is an integral component of the ring in the 6S complex, while Gemin2 and SMN occupy more distal positions on the convex face of an opened ring in the 7S complex.

The SMN Complex Is a Catalyst of SnRNP Core Formation

SnRNP core formation, albeit a thermodynamically favorable reaction (Raker et al., 1996), depends on PRMT5 and SMN complexes in vivo (Meister et al., 2002; Paushkin et al., 2002). We reasoned that these *trans*-acting factors are required to modulate the energetics of key steps of this reaction. To address this hypothesis, we deduced the energy profile of the in vivo Sm core assembly reaction, taking the reaction intermediates described in Figures 1–5 into account. First, we considered the energy levels of newly synthesized Sm proteins (the substrates of the reaction) and the assembled Sm core (the product of the reaction). Assuming that snRNP assembly in cells is, likewise, a spontaneous reaction, we suggest that free Sm proteins must occupy high energy levels along the reaction coordinate, whereas the Sm core would reflect a global energetic minimum. The 6S complex must reside in a local minimum along the reaction coordinate since it is stable under steady-state conditions in extracts. We further postulate that Sm proteins are inhibited from forming Sm cores out of the pICln-bound state due to a very high activation energy barrier (Figure 6A, blue line). On the basis of experiments shown in Figures 3 and 4, we propose that the SMN complex helps Sm proteins surmount this unfavorable energetic obstacle (Figure 6A, green line). A consequence of these arguments is that, first, the SMN complex loaded with Sm proteins occupies another local yet transient energetic minimum and, second, that the SMN complex acts as a catalyst for snRNP assembly.

Two strategies were employed to test this assumption experimentally. The first relied on the observation that snRNP cores are exceedingly stable structures, capable of withstanding treatment with 7 M urea or 2.5 M NaCl (Liautard et al., 1982). Thus, spontaneous exchange of Sm proteins from an assembled snRNP core to a free snRNA is unlikely (Figure 6B, top panel). However, if the prediction of our energetic considerations holds true, the exchange of Sm proteins should be possible upon addition of a molar excess of the SMN complex over the Sm proteins of the snRNP (Figure 6B, bottom panel). As concentrated solutions of catalyst are required for this type of experiment, we used recombinant SMNΔGemin3–5 complex rather than the endogenous SMN complex. Indeed, addition of an 8-fold molar excess of SMNΔGemin3–5 caused a half-maximal exchange of Sm proteins from the preformed snRNP to the unlabeled RNA (Figure 6C, lane 6), with a total exchange at a 30-fold molar excess (Figure 6C, lane 8). This effect was strictly dependent on the SMN and Gemin2 subunits of the SMN complex, as incubation with unlabeled RNA alone (Figure 6C, lanes 3 and 12) or with nonrelevant proteins in the presence of unlabeled RNA had no effect on the stability of the Sm core

and E/F/G, corresponding to single-turnover conditions. A control assembly reaction with 10 pmol 6S complex and RNA incubated in the absence of the SMNΔGemin3–5 complex is shown in panel III. The bottom panel shows quantification of the experiments. Data are represented as mean ± SD (n = 3).

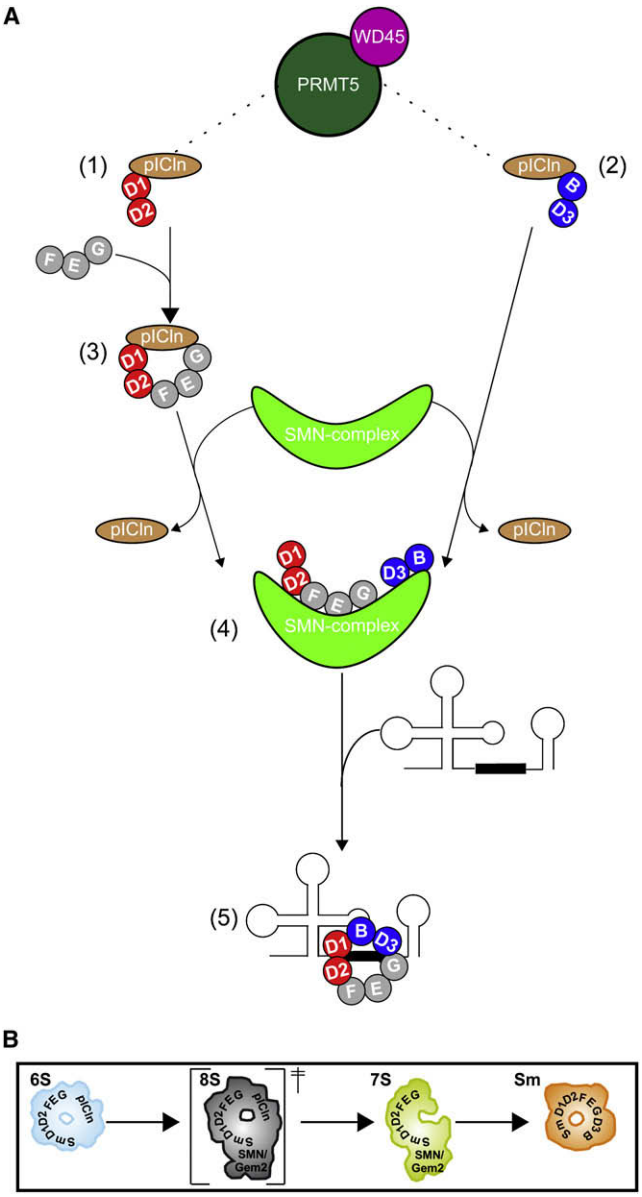

Figure 7. Model of the Assisted Assembly of SnRNPs and Structures of Key Intermediates

(A) The chaperone pICln initially binds D1/D2 and D3/B (1 and 2). EFG is then recruited to pICln/D1/D2 to form the 6S complex (3). Transfer of pICln-bound Sm proteins onto the SMN complex coincides with displacement of pICln and forms the loaded SMN complex (4). The SMN complex then allows RNA binding, ring closure, and RNP release (5).

(B) Structural EM models of intermediates of the assembly reaction. 6S (see also A3) forms a closed ring, 7S holds the Sm proteins in an open configuration (part of A4), and 8S represents a trapped transition complex from A3 to A4. The assembled core is derived from EM models of negatively stained snRNP cores.

(Figure 6C, lanes 13–18; see also Figure S8 for additional experiments). Of note, this reaction followed dose-dependent saturation kinetics (data not shown).

In the second approach, we asked whether the SMN complex is a catalyst of assembly reaction even when present in substoichiometric amounts and is, thus, capable of multiple turnover reactions. To test this possibility, we initially incubated a small amount of SMN complex (0.5 pmol) loaded with Sm proteins with a 20-fold molar excess of U1snRNA. To visualize the assembly reaction in native gels, 0.5% of the RNA substrate was radiolabeled. Under these conditions, the SMN complex delivered its Sm proteins onto the U1snRNA. However, due to the small amount of substrate (i.e., Sm proteins) used in this assay and the low specific activity of the U1snRNA, only marginal assembly could be observed (Figure 6D, panel II and lower panel green line). However, upon addition of a 20-fold molar excess (10 pmol) of the 6S complex, assembly was stimulated in a time-dependent manner (Figure 6D, panel I and lower panel blue line). Under these conditions, 2 pmol RNPs were generated per hour, directly showing multiple turnover of the substrate (Sm proteins and snRNA) to product. No assembly was observed when 6S was incubated with U1snRNA alone, showing the dependence of this reaction on the SMN complex (Figure 6D, panel III and lower panel red line). We conclude that the SMN complex facilitates snRNP assembly by (1) lowering the activation energy of the reaction from 6S to snRNP and (2) loading Sm proteins onto snRNA in a multiple turnover reaction. These results are consistent with a function of the SMN complex as a catalyst of snRNP formation.

DISCUSSION

In this study, we have applied a combination of biochemical and structural approaches to decipher key steps in the assisted assembly of snRNPs. We show that an assembly chaperone, pICln, initially induces the formation of otherwise unstable higher-order Sm protein complexes. In this state, a kinetic trap is imposed on the Sm proteins by bound pICln, which actively prevents their premature association with snRNA. Sm protein progression toward the snRNP core is mediated by the SMN complex that dissociates the inhibitory chaperone and catalyzes ring closure on snRNA. Our postulated mechanism is schematically depicted in Figure 7.

pICln Is an Assembly Chaperone for Sm Proteins

pICln has been described as a component of the PRMT5 complex that recruits Sm protein substrates to the methyltransferase PRMT5 (Friesen et al., 2001; Meister et al., 2001b). Our data reveal a second function for pICln as an organizer of assembly intermediates. The most stable complex contains the Sm proteins D1/D2 and E/F/G, which are tethered upon pICln binding into an RNA-free ring structure (Figure 7A, complex 3). Importantly, the resulting Sm-heteropentamer cannot form in the absence of pICln, as D1/D2 and E/F/G have little affinity for each other in the absence of snRNA (Raker et al., 1996). How does pICln induce the formation of this otherwise unstable Sm-heteropentamer? The solution structure of an N-terminal fragment of pICln shows that it adopts a fold with several antiparallel β strands, designated as a pleckstrin homology domain (Furst et al., 2005). Sm proteins have been reported to associate with each other by antiparallel β strands (Kambach et al., 1999). Thus, we suggest that pICln in the RNA-free 6S complex acts as a structural counterpart of D3/B in the assembled Sm core domain

(Kambach et al., 1999; Stark et al., 2001). The architecture of the 6S complex as determined by electron microscopy is consistent with this hypothesis; however, the validation of this model awaits the elucidation of high-resolution structures.

Pulse-chase experiments performed by G. Blobel and coworkers demonstrated an RNA-free 6S precursor of snRNP cores more than two decades ago (Fisher et al., 1985). This precursor was reported to form early in biogenesis and contained the Sm proteins E, F, G, and D (only one D protein was known at that time). Based on its apparent sedimentation coefficient, composition, and role in assembly, the pICln/D1/D2/E/F/G complex described here might be identical to this long-sought precursor.

pICln formed a second complex containing D3/B in vitro (Figure 7A, complex 2), which could not be isolated from cellular extracts as a separate entity. However, the Sm proteins D3/B are abundantly present in the isolated 20S PRMT5 complex (Figure 1B). Hence, we believe that pICln/D3/B is also formed in vivo but cannot be detected in extracts in steady state because it is either short lived or remains stably bound to the methyltransferase complex.

Consistent with studies in *Xenopus laevis* oocytes (Pu et al., 1999), we find Sm proteins incompetent of forming snRNPs in a pICln-bound state. The architecture of the 6S particle suggests that pICln sterically prevents the RNA from gaining access to its binding site on the inside of the Sm ring (Kambach et al., 1999; Stark et al., 2001; Urlaub et al., 2001). Based on the capability to promote higher-order assemblies and to simultaneously prevent premature RNA binding, pICln is an assembly chaperone specific for Sm proteins. Although similar factors have been described for the assembly of protein complexes (Hirano et al., 2006; Laskey et al., 1978; Le Tallec et al., 2007; Saschenbrecker et al., 2007), to our knowledge, pICln is the first protein of this class implicated in the assembly of RNPs. We predict that other RNPs containing Sm proteins in their cores, such as the U7snRNP, likewise require pICln as an assembly chaperone (Pillai et al., 2003).

The SMN Complex Acts as a Catalyst to Resolve a Kinetic Trap in Assembly

We have previously reported that the SMN complex is copurified upon immunopurification of pICln from assembly-active extracts, albeit in a substoichiometric manner (Meister and Fischer, 2002). This finding suggested Sm proteins to be transferred directly from pICln to the SMN complex. Indeed, here, we show that the SMN complex accepts Sm proteins from both 6S and pICln/D3/B complexes and simultaneously dissociates pICln. As a consequence of this reaction, Sm proteins regain the competence to form snRNP particles. Of note, neither the two other subunits of the PRMT5 complex nor arginine methylation of Sm proteins appears to be essential for Sm protein transfer onto the SMN complex in vitro. However, we do not exclude at this stage that this posttranslational modification might modulate the kinetics or efficiency of this reaction.

We suggest that the failure of Sm proteins to interact with snRNA as part of the 6S complex is associated with a very high activation energy barrier in the transition from 6S to the assembled snRNP (Figure 6A). The capability of the SMN complex to accept Sm proteins from this state and transfer them onto RNA implies that it lowers this energetic hurdle and, therefore, is a catalyst of the reaction (Figure 6A). In favor of this idea, a moderate molar excess of the SMN complex was capable of melting a preformed snRNP core, an exceedingly thermodynamically stable entity (Liautard et al., 1982). Furthermore, the SMN complex acts substoichiometrically in snRNP formation and, hence, exhibits multiple turnover (Figure 6D). These findings indicate that snRNP assembly is a catalyzed reaction in vivo, with the SMN complex bound to Sm proteins, representing a transition-state intermediate (Figure 7A, complex 4). Considering the high abundance of Sm proteins in the cytoplasm, the nuclear export of snRNA is likely to be the global rate-limiting step of snRNP assembly. This unbalanced availability of both substrates may explain the stability of the SMN complex under steady-state conditions.

An SMN complex composed of only SMN and Gemins 2 and 8 appears to be sufficient for both aforementioned activities (Figures 3 and 4). However, performing the transfer reaction with Gemin2/SMNΔC has allowed us to uncouple 6S complex binding and pICln release (Figure 3B). Also, this complex failed to efficiently accept pICln/D3/B (Figure 3B). From these experiments, we conclude that either Gemin8 and/or the C-terminal portion of SMN affects pICln release and, simultaneously, constitutes the binding site for Sm D3/B.

We obtained further mechanistic insight into the role of the SMN complex in snRNP core formation by electron microscopy of assembly intermediates (Figure 5). When the architecture of the stalled 8S transfer intermediate was compared to 6S and 7S complexes, we found that SMN and Gemin2 occupy positions on the outer face of the pICln-Sm protein ring. Thus, the transfer reaction relieves Sm proteins of the pICln-imposed steric hindrance and enables the RNA to access its binding site on the inner face of the Sm protein ring. How is pICln dissociation affected? Binding of the SMN complex onto the outer surface of the 6S ring may induce a conformational change in the Sm proteins of the 6S complex that results in pICln release. The SMN complex then holds Sm proteins in an open-ring configuration, poised for transfer onto snRNA. These findings also suggest that the spatial organization of Sm proteins in the snRNP is attained already at the level of the 6S complex, i.e., in an early stage of assembly (Figure 7B).

Structural Similarity of SnRNP Assembly with DNA-Clamp Loading

Based on our studies, we hypothesize that the SMN complex-assisted formation of snRNPs is structurally similar to the clamp-loading reaction, i.e., the process by which ring-shaped clamps are placed onto DNA to tether poorly processive DNA replication enzymes (Ellison and Stillman, 2001; Indiani and O'Donnell, 2006). Clamp loaders are hetero-oligomeric protein assemblies that bind and open hexameric clamp rings in an ATP-dependent manner. ATP hydrolysis then induces a conformational change in the loader, which leads to ring closure and ejects the clamp onto DNA (Davey et al., 2002; Johnson and O'Donnell, 2005). What then are the similarities to the formation of snRNP cores? The Sm core is a toroidal RNP (Kambach et al., 1999; Stark et al., 2001) and is thus structurally similar to

a replication clamp around DNA (Georgescu et al., 2008). The SMN complex holds the Sm proteins in an open state poised for transfer onto RNA (Figure 7B), reminiscent of the clamp-loading complex. Although the eight subunits making up the SMN complex and ATP are required in cells, a minimal complex composed of SMN and Gemin2 is sufficient to catalyze formation of the snRNP core in vitro in the absence of ATP. Similarly, a minimal *E. coli* clamp loader consisting of the δ subunit only transfers clamps onto DNA without a nucleotide requirement. Thus, it is intriguing to postulate that cells have evolved two separate machineries to deal with a similar topological problem in the joining of nucleic acids with proteins. Future studies will elucidate fine-tuning and regulation of this reaction.

EXPERIMENTAL PROCEDURES

Sm Protein Transfer Assays

Fifty picomoles of the indicated SMN complex were immobilized to 20 μl of an anti-SMN resin. One hundred picomoles of either 6S or pICln/D3/B complex were added and incubated at 37°C for 1 hr. After washing with 3 × 1 ml PBS, the retained proteins were eluted with SDS-PAGE loading buffer. 50% of this eluate was analyzed by SDS-PAGE. The rest was subjected to western blotting with both anti-pICln and anti-Gemin2 as a loading control.

Sm Protein Strand Exchange Assays

Sm cores were preformed using 3 pmol Sm proteins and 0.3 pmol ^{32}P-labeled snRNA as described (Raker et al., 1996). To this, 100 pmol of unlabeled Sm site oligonucleotide (AAUUUUUGA) and increasing amounts of SMNΔGemin3–5 complex were added. After incubation for 2.5 hr at 37°C, the mixtures were analyzed by native gel electrophoresis as described (Meister et al., 2001a). The indicated SMNΔGemin3–5 molar excesses over the Sm proteins were used.

Reconstitution of Sm Protein-Containing Complexes

Due to the strongly contrasting pI values of the assembly factors (pICln, SMN, and Gemin2) and Sm proteins, direct mixture of these proteins resulted in irreversible aggregation. To circumvent this, the respective proteins were mixed in 20 mM HEPES-NaOH (pH 7.5), 1 M NaCl, and 5 mM DTT and dialyzed overnight to 20 mM HEPES-NaOH (pH 7.5), 0.2 M NaCl, and 5 mM DTT at 4°C. Complex formation was then monitored by gel filtration run in 20 mM HEPES-NaOH (pH 7.5), 0.2 M NaCl, and 5 mM DTT, using a Superdex200 10/300 column (GE Healthcare) and subsequent SDS-PAGE of individual fractions.

Electron Microscopy and Single-Particle Image Processing

For EM sample preparation, purified complexes were subjected to the GraFix approach using a 5%–20% glycerol gradient (Kastner et al., 2008), and specimens were negatively stained with uranyl formate according to a previously published protocol (Golas et al., 2003). Images were taken on a Philips CM200 electron microscope (Philips/FEI, Eindhoven, The Netherlands) using a 4-fold binned 4 k × 4 k CCD camera (TemCam-F415, TVIPS, Gauting, Germany) at a magnification of 343,000- and 380,000-fold (Sander et al., 2005). 42014, 11126, 31150, and 27131 single-particle images were selected for the data sets of the 6S, 8S (6S+SMN/Gemin2), 8S (7S+pICln), and 7S complex, respectively. Using iteratively refined class averages, single-particle images were aligned via an exhaustive polar alignment (Sander et al., 2003) and subsequent multivariate statistical analysis (MSA)-based hierarchical ascendant classification (HAC) in the context of IMAGIC-5 (van Heel et al., 1996) into classes of 35–40 class members in average. All four data sets were processed independently of the other three; at no state of image analysis were the results of one data set used to refine another. After four iterations, the results were stable. Representative class averages were selected for presentation, and difference maps were calculated from the normalized, bandpass-filtered class averages using IMAGIC-5.

Additional Experimental Procedures can be found in the Supplemental Data.

SUPPLEMENTAL DATA

The Supplemental Data include Supplemental Discussion, Experimental Procedures, eight figures, and two tables and can be found with this article online at http://www.cell.com/supplemental/S0092-8674(08)01177-X.

ACKNOWLEDGMENTS

We thank T. Müller, P. Stayton, C. Kambach, J. Steitz, and I. Mattaj for reagents; J. Ohmer for technical assistance; and B. Laggerbauer, M. Kroiss, G. Matera, S. Jentsch, S. Rospert, F.U. Hartl, and R. Lührmann for comments. This work was supported by grants of the DFG (SFB581, TP B18) and AFM (ID11730) to U.F. and grants of the BMBF and European "3D Repertoire" to H.S.

Received: April 25, 2008
Revised: July 14, 2008
Accepted: September 8, 2008
Published: October 30, 2008

REFERENCES

Brahms, H., Meheus, L., de Brabandere, V., Fischer, U., and Lührmann, R. (2001). Symmetrical dimethylation of arginine residues in spliceosomal Sm protein B/B′ and the Sm-like protein LSm4, and their interaction with the SMN protein. RNA *7*, 1531–1542.

Davey, M.J., Jeruzalmi, D., Kuriyan, J., and O'Donnell, M. (2002). Motors and switches: AAA+ machines within the replisome. Nat. Rev. Mol. Cell Biol. *3*, 826–835.

Ellison, V., and Stillman, B. (2001). Opening of the clamp: an intimate view of an ATP-driven biological machine. Cell *106*, 655–660.

Fischer, U., Liu, Q., and Dreyfuss, G. (1997). The SMN-SIP1 complex has an essential role in spliceosomal snRNP biogenesis. Cell *90*, 1023–1029.

Fisher, D.E., Conner, G.E., Reeves, W.H., Wisniewolski, R., and Blobel, G. (1985). Small nuclear ribonucleoprotein particle assembly *in vivo*: demonstration of a 6S RNA-free core precursor and posttranslational modification. Cell *42*, 751–758.

Friesen, W.J., and Dreyfuss, G. (2000). Specific sequences of the Sm and Sm-like (Lsm) proteins mediate their interaction with the spinal muscular atrophy disease gene product (SMN). J. Biol. Chem. *275*, 26370–26375.

Friesen, W.J., Paushkin, S., Wyce, A., Massenet, S., Pesiridis, G.S., Van Duyne, G., Rappsilber, J., Mann, M., and Dreyfuss, G. (2001). The methylosome, a 20S complex containing JBP1 and pICln, produces dimethylarginine-modified Sm proteins. Mol. Cell. Biol. *21*, 8289–8300.

Furst, J., Schedlbauer, A., Gandini, R., Garavaglia, M.L., Saino, S., Gschwentner, M., Sarg, B., Lindner, H., Jakab, M., Ritter, M., et al. (2005). ICln159 folds into a pleckstrin homology domain-like structure. Interaction with kinases and the splicing factor LSm4. J. Biol. Chem. *280*, 31276–31282.

Georgescu, R.E., Kim, S.S., Yurieva, O., Kuriyan, J., Kong, X.P., and O'Donnell, M. (2008). Structure of a sliding clamp on DNA. Cell *132*, 43–54.

Golas, M.M., Sander, B., Will, C.L., Lührmann, R., and Stark, H. (2003). Molecular architecture of the multiprotein splicing factor SF3b. Science *300*, 980–984.

Gubitz, A.K., Feng, W., and Dreyfuss, G. (2004). The SMN complex. Exp. Cell Res. *296*, 51–56.

Hirano, Y., Hayashi, H., Iemura, S., Hendil, K.B., Niwa, S., Kishimoto, T., Kasahara, M., Natsume, T., Tanaka, K., and Murata, S. (2006). Cooperation of multiple chaperones required for the assembly of mammalian 20S proteasomes. Mol. Cell *24*, 977–984.

Indiani, C., and O'Donnell, M. (2006). The replication clamp-loading machine at work in the three domains of life. Nat. Rev. Mol. Cell Biol. *7*, 751–761.

Johnson, A., and O'Donnell, M. (2005). Cellular DNA replicases: components and dynamics at the replication fork. Annu. Rev. Biochem. *74*, 283–315.

Kambach, C., Walke, S., Young, R., Avis, J.M., de la Fortelle, E., Raker, V.A., Lührmann, R., Li, J., and Nagai, K. (1999). Crystal structures of two Sm protein complexes and their implications for the assembly of the spliceosomal snRNPs. Cell *96*, 375–387.

Kastner, B., and Lührmann, R. (1989). Electron microscopy of U1 small nuclear ribonucleoprotein particles: shape of the particle and position of the 5′ RNA terminus. EMBO J. *8*, 277–286.

Kastner, B., Fischer, N., Golas, M.M., Sander, B., Dube, P., Boehringer, D., Hartmuth, K., Deckert, J., Hauer, F., Wolf, E., et al. (2008). GraFix: sample preparation for single-particle electron cryomicroscopy. Nat. Methods *5*, 53–55.

Kroiss, M., Schultz, J., Wiesner, J., Chari, A., Sickmann, A., and Fischer, U. (2008). Evolution of an RNP assembly system: A minimal SMN complex facilitates formation of UsnRNPs in *Drosophila melanogaster*. Proc. Natl. Acad. Sci. USA *105*, 10045–10050.

Laskey, R.A., Honda, B.M., Mills, A.D., and Finch, J.T. (1978). Nucleosomes are assembled by an acidic protein which binds histones and transfers them to DNA. Nature *275*, 416–420.

Le Tallec, B., Barrault, M.B., Courbeyrette, R., Guerois, R., Marsolier-Kergoat, M.C., and Peyroche, A. (2007). 20S proteasome assembly is orchestrated by two distinct pairs of chaperones in yeast and in mammals. Mol. Cell *27*, 660–674.

Liautard, J.P., Sri-Widada, J., Brunel, C., and Jeanteur, P. (1982). Structural organization of ribonucleoproteins containing small nuclear RNAs from HeLa cells. Proteins interact closely with a similar structural domain of U1, U2, U4 and U5 small nuclear RNAs. J. Mol. Biol. *162*, 623–643.

Massenet, S., Pellizzoni, L., Paushkin, S., Mattaj, I.W., and Dreyfuss, G. (2002). The SMN complex is associated with snRNPs throughout their cytoplasmic assembly pathway. Mol. Cell. Biol. *22*, 6533–6541.

Meister, G., and Fischer, U. (2002). Assisted RNP assembly: SMN and PRMT5 complexes cooperate in the formation of spliceosomal UsnRNPs. EMBO J. *21*, 5853–5863.

Meister, G., Bühler, D., Pillai, R., Lottspeich, F., and Fischer, U. (2001a). A multiprotein complex mediates the ATP-dependent assembly of spliceosomal U snRNPs. Nat. Cell Biol. *3*, 945–949.

Meister, G., Eggert, C., Bühler, D., Brahms, H., Kambach, C., and Fischer, U. (2001b). Methylation of Sm proteins by a complex containing PRMT5 and the putative U snRNP assembly factor pICln. Curr. Biol. *11*, 1990–1994.

Meister, G., Eggert, C., and Fischer, U. (2002). SMN-mediated assembly of RNPs: a complex story. Trends Cell Biol. *12*, 472–478.

Neuenkirchen, N., Chari, A., and Fischer, U. (2008). Deciphering the assembly pathway of Sm-class U snRNPs. FEBS Lett. *582*, 1997–2003.

Paushkin, S., Gubitz, A.K., Massenet, S., and Dreyfuss, G. (2002). The SMN complex, an assemblyosome of ribonucleoproteins. Curr. Opin. Cell Biol. *14*, 305–312.

Pellizzoni, L. (2007). Chaperoning ribonucleoprotein biogenesis in health and disease. EMBO Rep. *8*, 340–345.

Pellizzoni, L., Yong, J., and Dreyfuss, G. (2002). Essential role for the SMN complex in the specificity of snRNP assembly. Science *298*, 1775–1779.

Pillai, R.S., Grimmler, M., Meister, G., Will, C.L., Lührmann, R., Fischer, U., and Schümperli, D. (2003). Unique Sm core structure of U7 snRNPs: assembly by a specialized SMN complex and the role of a new component, Lsm11, in histone RNA processing. Genes Dev. *17*, 2321–2333.

Pu, W.T., Krapivinsky, G.B., Krapivinsky, L., and Clapham, D.E. (1999). pICln inhibits snRNP biogenesis by binding core spliceosomal proteins. Mol. Cell. Biol. *19*, 4113–4120.

Raker, V.A., Plessel, G., and Lührmann, R. (1996). The snRNP core assembly pathway: identification of stable core protein heteromeric complexes and an snRNP subcore particle *in vitro*. EMBO J. *15*, 2256–2269.

Sander, B., Golas, M.M., and Stark, H. (2003). Corrim-based alignment for improved speed in single-particle image processing. J. Struct. Biol. *143*, 219–228.

Sander, B., Golas, M.M., and Stark, H. (2005). Advantages of CCD detectors for de novo three-dimensional structure determination in single-particle electron microscopy. J. Struct. Biol. *151*, 92–105.

Saschenbrecker, S., Bracher, A., Rao, K.V., Rao, B.V., Hartl, F.U., and Hayer-Hartl, M. (2007). Structure and function of RbcX, an assembly chaperone for hexadecameric Rubisco. Cell *129*, 1189–1200.

Shpargel, K.B., and Matera, A.G. (2005). Gemin proteins are required for efficient assembly of Sm-class ribonucleoproteins. Proc. Natl. Acad. Sci. USA *102*, 17372–17377.

Stark, H., Dube, P., Lührmann, R., and Kastner, B. (2001). Arrangement of RNA and proteins in the spliceosomal U1 small nuclear ribonucleoprotein particle. Nature *409*, 539–542.

Urlaub, H., Raker, V.A., Kostka, S., and Lührmann, R. (2001). Sm protein-Sm site RNA interactions within the inner ring of the spliceosomal snRNP core structure. EMBO J. *20*, 187–196.

van Heel, M., Harauz, G., Orlova, E.V., Schmidt, R., and Schatz, M. (1996). A new generation of the IMAGIC image processing system. J. Struct. Biol. *116*, 17–24.

Will, C.L., and Lührmann, R. (2001). Spliceosomal UsnRNP biogenesis, structure and function. Curr. Opin. Cell Biol. *13*, 290–301.

Winkler, C., Eggert, C., Gradl, D., Meister, G., Giegerich, M., Wedlich, D., Laggerbauer, B., and Fischer, U. (2005). Reduced U snRNP assembly causes motor axon degeneration in an animal model for spinal muscular atrophy. Genes Dev. *19*, 2320–2330.

Zhang, Z., Lotti, F., Dittmar, K., Younis, I., Wan, L., Kasim, M., and Dreyfuss, G. (2008). SMN deficiency causes tissue-specific perturbations in the repertoire of snRNAs and widespread defects in splicing. Cell *133*, 585–600.